PHYSICAL REVIEW B

SOLID STATE

THIRD SERIES, VOL. 2, NO. 4 15 AUGUST 1970

Annealing of Quenched Defects in Gold†

J. J. Burton* and D. Lazarus
Department of Physics and Materials Research Laboratory, University of Illinois, Urbana, Illinois 61801
(Received 8 October 1969; revised manuscript received 2 March 1970)

The slope-change method for determination of activation energies of migrating defects is examined using computer-generated data based on a simplified model of the annealing of quenched gold. It is shown that there are two well-defined activation energies. One is the instantaneous activation energy which is characteristic of the defect-annihilating step. The second is the apparent activation energy which is characteristic of the rate-limiting annealing step. The two activation energies can be obtained only if accurate time derivatives of the defect concentration are examined. These ideas are applied to the annealing of high-purity gold quenched from 975 °C. The resistance-annealing curves and their first and second derivatives are studied using a new measuring technique which yields continuous plots of the resistance. The annealing curves are consistent with a simple model involving single vacancies, divacancies, and a time-dependent sink concentration. The instantaneous activation energy is 0.52 ± 0.03 eV and is identified with the divacancy-motion energy. The apparent activation energy is between 0.70 and 0.95 eV.

I. INTRODUCTION

Quenching experiments are used extensively to examine the behavior of defects in metals. In these experiments, an excess of defects is produced and then allowed to anneal out. The decay of the excess defects is followed by measuring changes in a defect-dependent observable. The decay data are then analyzed in an attempt to gain insight into the fundamental atomic processes involved in the formation, motion, and annihilation of the defects.

Several investigators have studied the possible reactions involved in annealing of point defects.[1–4] Johnson[5] has used a computer to simulate complicated annealing processes and has shown that the data are not readily related to the assumed processes. There is considerable interest in analyzing annealing data, and several authors have discussed the assumptions made in various analysis procedures.[6–8] However, there has been very little investigation of the results obtained with these procedures in cases where the atomic processes are known.[7]

In this paper, we investigate one data-analysis procedure, the widely employed slope-change method for determination of activation energies. We show that a study of the time derivatives of the excess-defect concentration may make it possible to obtain not one, but two quite distinct activation energies: an instantaneous energy and an apparent energy. The instantaneous energy is shown to be characteristic of the actual defect-annihilation processes whereas the apparent energy is shown to be related to the rate-controlling processes. Conventional slope-change data,[9] which use only the defect concentration, yield a single activation energy which is intermediate between the instantaneous and apparent energies and is not necessarily characteristic of any single microscopic process. These conclusions are illustrated with a simplified theoretical model of the annealing of quenched gold and are then applied to experimental data on gold.

The annealing of quenched gold was chosen for this study as it has been studied extensively since the early work of Kauffman and Koehler.[10] Despite many experiments and models proposed for

the annealing process,[11] there remains some uncertainty as to the explanation of the experimental results. Identifications of the observed activation energies are frequently conflicting,[12,13] and the details of the shape of the annealing curve have not been examined.

Our examination of the slope-change procedure indicates that time derivatives of the quenched-in resistance are required in order to understand the annealing processes. Resistance-annealing data obtained continuously with the sample maintained at constant temperature in the annealing bath can provide continuous time derivatives. Such information is not obtainable from data derived by periodically making resistance measurements with the specimen as it is quenched from the annealing temperature into liquid helium.

We have used a simple differential circuit, originally developed by Bourassa *et al.*[14,15] to make continuous measurements, during annealing, of the defect resistance of 16-mil wires of 99 9999% gold, fast quenched from 975 °C. The data are differentiable, and continuous first and second derivatives are obtained.

The data are consistent with a model based on single vacancies, divacancies, and sinks whose concentration is increasing at small times. The instantaneous activation energy is found to be 0.52 ± 0.3 eV and is identified with the divacancy-motion energy. This value of the divacancy-motion energy differs from that reported by other investigators.[12] The apparent activation energy is between 0.70 and 0.95 eV; no attempt is made to identify it at this time. Some preliminary results of this study have been published elsewhere.[16]

II. SLOPE-CHANGE METHOD

The slope-change method of analysis has been discussed previously.[6-8] We review it briefly in this section.

For a *single* thermally activated annealing process where the observable parameter is ρ, we may write

$$\frac{d\rho}{dt} = f(\rho) e^{-E/kT}, \tag{1}$$

where E is the activation energy, k is Boltzmann's constant, and T is the annealing temperature. From Eq. (1) the activation energy is evidently defined as

$$E = -k \frac{d}{d(1/T)} \ln \frac{d\rho}{dt}. \tag{2}$$

The so-called slope-change method is based on Eq. (2). Experimentally, the sample is held at temperature T_1 and annealed; suddenly, at a time t_0, its temperature is changed to T_2, and the annealing rate is changed. In this case the activation energy E is given by

$$E = k \frac{T_1 T_2}{T_2 - T_1} \ln\left(\frac{d\rho}{dt}(T_2, t_0) \Big/ \frac{d\rho}{dt}(T_1, t_0) \right). \tag{3}$$

Since both slopes are measured at the same time t_0, the defect concentrations are presumed to be the same at both determinations.

In practice, the data are not obtained instantaneously as assumed above. The parameter ρ is usually measured at discrete time intervals beginning some time after t_0, and $d\rho(t_0)/dt$ cannot be obtained readily. A smooth curve is usually drawn through the measured values of $\rho(t)$, and $d\rho(t_0)/dt$ can only be estimated by extrapolation to t_0 from this smooth curve. There are inherent problems in determining the slope of a curve at its end point and so, unless the shape of $\rho(t)$ is known in advance, $d\rho(t_0)/dt$ may not be well determined. These problems may be surmounted by measuring ρ continuously, rather than discretely, and thereby obtaining accurate time derivatives of ρ.

There is a more basic problem in the use of Eq. (3) to determine E. In general, we cannot expect that annealing is a single thermally activated process, as assumed in Eq. (1), and so the assumptions leading to Eq. (3) are violated.[7] For more complicated annealing processes, it is still possible to define operationally an effective activation energy E_{eff} from Eq. (3). However, this E_{eff} is not necessarily closely relatable to fundamental atomic processes. We shall use simpler computer-simulated annealing curves to investigate the relation between the activation energy, thus calculated, and the microscopic behavior of the defects.

III. SLOPE-CHANGE SIMULATION

A. Model

We use here a simplified model of the annealing of quenched gold based on single vacancies V_1, divacancies V_2, and fixed sinks S. The following reactions can occur[17,18]:

$$V_1 + V_1 \underset{k_{21}}{\overset{k_{12}}{\rightleftharpoons}} V_2, \quad V_1 + S \xrightarrow{k_1} S, \quad V_2 + S \xrightarrow{k_2} S. \tag{4}$$

The model gives the following coupled differential equations connecting V_1, V_2, and S:

$$\begin{aligned} \frac{dV_1}{dt} &= -k_{12} V_1^2 - k_1 V_1 S + k_{21} V_2, \\ \frac{dV_2}{dt} &= -\tfrac{1}{2} k_{21} V_2 - k_2 V_2 S + \tfrac{1}{2} k_{12} V_1^2, \end{aligned} \tag{5}$$

where for the fcc lattice

$$k_{12}=84\nu e^{-E_1^m/kT},\quad k_1=12\nu e^{-E_1^m/kT},$$
$$k_{21}=14\nu e^{-(E_1^m+B_2)/kT},\quad k_2=8\nu e^{-E_2^m/kT}. \tag{6}$$

Here E_1^m is the single-vacancy-motion energy, E_2^m is the divacancy-motion energy, and B_2 is the divacancy-binding energy. We neglect differing entropy terms. For discussion purposes in this paper, we first assume that the parameters have values[12]

$$E_1^m=0.90\text{ eV},\quad E_2^m=0.70\text{ eV},\quad B=0.40\text{ eV}. \tag{7}$$

We shall show later that these values are not consistent with our experimental results. This conclusion does not affect the present discussion. We also assume a constant value for the frequency factor[19]

$$\nu=10^{14}\text{ min}^{-1}, \tag{8}$$

and, for the moment, that divacancies, once formed, are stable and are the only defects moving to sinks, so that

$$k_1=k_{21}=0. \tag{9}$$

We finally assume that the experimental observable is the total vacancy concentration given by

$$R=V_1+2V_2. \tag{10}$$

Thus, from (5) and (10), with assumption (9)

$$\frac{dR}{dt}=\frac{dV_1}{dt}+\frac{2dV_2}{dt}=-2k_2V_2S. \tag{11}$$

In the present model, the divacancies running to sinks comprise the only directly observable annealing process. Note that if the sink density S is sufficiently large, the rate-limiting step in this reaction scheme is the formation of divacancies from single vacancies, which determines the concentration V_2. However, if S is small enough, the rate-limiting step is the divacancies moving to sinks, as expressed by the factor k_2.

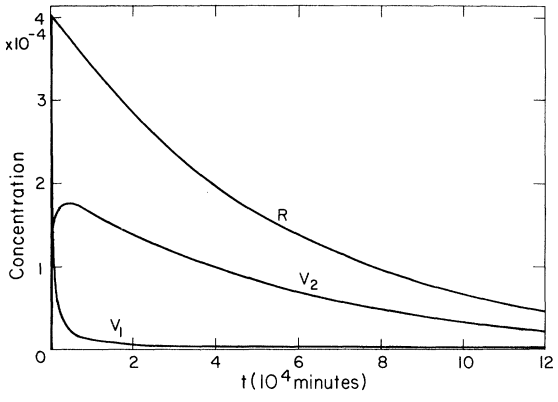

FIG. 1. Total vacancy concentration R, single-vacancy concentration V_1, and divacancy concentration V_2 versus time for annealing with a low sink concentration of 10^{-8}.

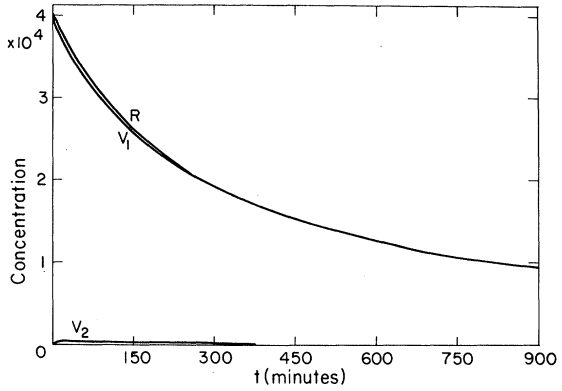

FIG. 2. Total vacancy concentration R, single-vacancy concentration V_1, and divacancy concentration V_2 versus time for annealing with a high sink concentration of 10^{-4}.

We have solved Eq. (5) with our assumptions at $T=303$ °K by computer simulation with the initial conditions $V_1(0)=4\times10^{-4}$ and $V_2(0)=0$ for two limiting cases of large and small sink density. The initial conditions for V_1 and V_2 correspond roughly to gold rapidly quenched from about 975 °C.[20] Figure 1 shows the time dependence of R, V_1, and V_2 for $S=10^{-8}$, a very low sink concentration. Figure 2 shows the behavior of the same variables for $S=10^{-4}$, a very high sink concentration. In the low sink concentration case (Fig. 1) the annealing half-time is long (~40 000 min), the vacancies are mostly divacancies, and the annealing curve is almost first order. In the high sink concentration case (Fig. 2) the annealing half-time is short (~300 min), nearly all of the vacancies are single vacancies, and the annealing curve is almost second order.

A slope-change run is made experimentally by annealing at one fixed temperature T_1 and then abruptly changing the temperature to a new value T_2. This procedure is readily simulated on the computer. We begin our simulated slope-change run with approximately half the initial excess-defect resistance annealed out. The equations are then solved for the two extreme values of S with $T_1=303$ °K for 40 min and then with $T_2=313$ °K for an additional 40 min. The results of these slope-change experiments can best be seen by examining the two cases separately.

B. Low Sink Concentration

The slope-change curve for $S=10^{-8}$ is shown in

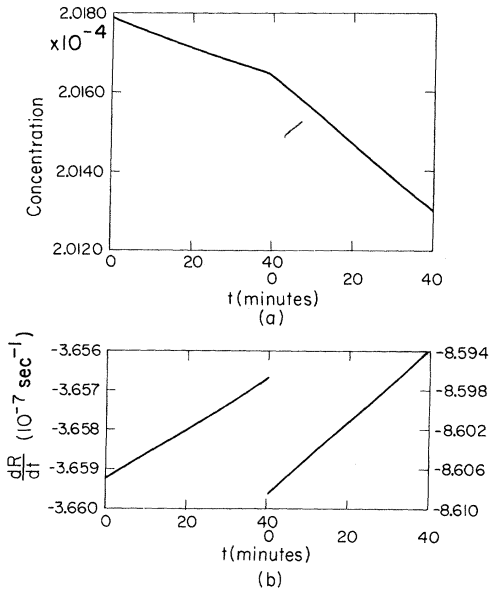

FIG. 3. Slope-change annealing for a low sink density. The first 40 min are at 303 °K and the second 40 min are at 313 °K. (a) The total vacancy concentration R, versus time; (b) dR/dt versus time.

Fig. 3(a). When the temperature is increased from 303 to 313 °K the defect concentration R decreases more rapidly. The first time derivative dR/dt is shown in Fig. 3(b). It is a monotonic function at both temperatures. Using the actual values of the slopes at $t = t_0$ in the slope-change equation [Eq. (3)], we derive an *instantaneous activation energy* of 0.70 eV. Extrapolation of the slopes from later times to t_0 gives us an *apparent activation energy*. In this case, since dR/dt is monotonic following t_0, the apparent activation energy is also 0.70 eV. In our model, this value corresponds to the activation energy for the motion of the divacancies to sinks, which is the defect-annihilating step as well as the rate-limiting step. In this slope-change run, nearly all the vacancies were in the form of divacancies before the temperature was changed (Fig. 1), and so the temperature change does not appreciably affect the divacancy concentration. Thus, only the divacancy-motion energy is observed for both instantaneous and apparent activation energies.

C. High Sink Concentration

The slope-change curve for $S = 10^{-4}$ is shown in Fig. 4(a) and the time derivative dR/dt is shown in Fig. 4(b). R decreases more rapidly after the temperature change than before it. However, dR/dt is not monotonic for this case. At the instant of temperature change, the relation between the single-vacancy, divacancy, and sink concentrations reflects the low-temperature distribution. Comparing annealing rates at the actual time of the temperature change, we again find an instantaneous activation of energy of 0.70 eV. This occurs because, in the model, the only directly observable defect-annihilation reaction is that of divacancies moving to sinks as described by Eq. (11). However, divacancies are formed faster at the higher temperature, and the annealing rate increases for a short time before falling off in the normal fashion because of decreasing total defect concentration. After the restabilization period during the first 5 min following the temperature change, the single vacancy and divacancies reach their proper relative concentrations at the new temperature, and dR/dt changes monotonically with time. It is possible to extrapolate these later values of dR/dt back to the time of the temperature change as shown in Fig. 4(b). From the value of the slope extrapolated to t_0, we may calculate an apparent activation energy from Eq. (11). In this case, the dR/dt curve extrapolated to $t = 0$ gives a value

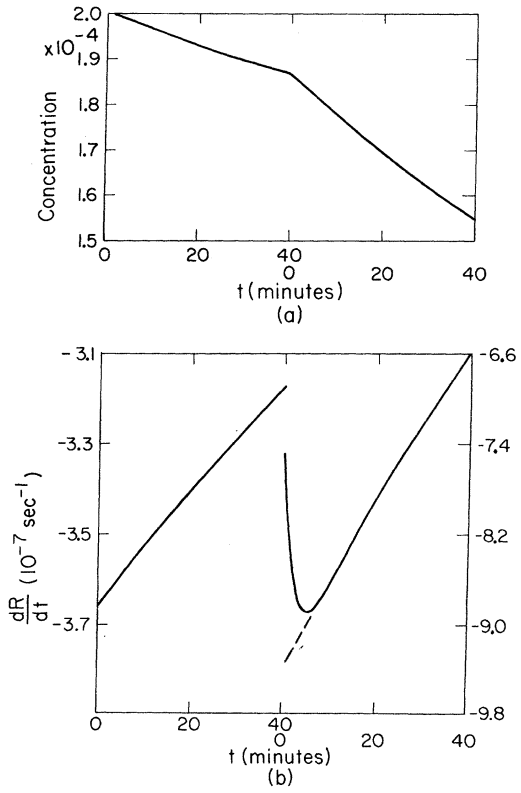

FIG. 4. Slope-change annealing for a high sink density. The first 40 min are at 303 °K and the second 40 min are at 313 °K. (a) The total vacancy concentration R versus time; (b) dR/dt versus time (left-hand scale, first 40 min; right-hand scale, second 40 min).

for the annealing rate at the time of the temperature change which might have been observed had the divacancies and single vacancies actually returned to local equilibrium fast enough. In Fig. 4, this extrapolation gives an apparent activation energy of 0.90 eV. This energy, the single-vacancy-motion energy, is observed since the divacancy concentration is very small and the formation of divacancies from single vacancies forms the rate-limiting step in the annealing process over long periods of time.

Thus, in slope-change experiments, there are two well-defined activation energies. The instantaneous activation energy, derived from the actual values of the annealing rates at time t_0, always corresponds to the energy of the annihilation step-divacancy motion in our model. The apparent activation energy, obtained by extrapolation of the annealing rate to time t_0, reflects the actual rate-limiting step. In our model of the annealing of quenched gold,[17,18] the single vacancies react to form divacancies and divacancies annihilate at sinks. The apparent activation energy corresponds to the divacancy-motion energy for very low sink concentrations, in which case divacancy motion is the rate-limiting step. However, for very high sink concentrations, divacancy formation is the rate-limiting step and the *single-vacancy*-motion energy is observed as the apparent activation energy. For intermediate sink densities, the apparent activation energy would be between the single-vacancy and divacancy-motion energies, while the instantaneous activation energy would always correspond to the divacancy-motion energy.

In conventional slope-change experiments,[9] data are taken at discrete time intervals, and time derivatives of the data are not obtained directly. The slope at the temperature-change time is determined by extrapolation from a smooth curve through the data points. In the very low sink concentration case, where the slope is monotonic and very regular, a proper activation energy can be obtained, since the apparent and instantaneous activation energies are identical. However, in the very high sink concentration case, the instantaneous and apparent activation energies may differ considerably, and the annealing rate may not be monotonic. In this case, the activation energy obtained by conventional slope-change measurements and extrapolation may be intermediate between the true instantaneous and apparent activation energies, since curve smoothing procedures tend to smooth the derivatives. These conclusions are demonstrated experimentally in Secs. IV–VI. Gold is fast quenched from high temperatures in order to obtain data corresponding roughly to our high sink case. It is shown that the instantaneous and apparent activation energies do indeed differ and that conclusions based on conventional experiments may be incorrect.

IV. EXPERIMENTAL

The samples were 16-mil wires of nominal 99.9999% gold, produced by Cominco. The size-corrected resistance ratios of the samples $R_{298°K}/R_{4°K}$ were about 4000. The total impurity content of the samples, as determined by Cominco after making the wires, was stated to be less than 0.3 ppm. The wire, as received, was analyzed at the University of Illinois with a high-resolution mass spectrograph, and the measured impurity content is shown in Table I. The impurity concentrations shown in the table were obtained by comparison with an N. B. S. standard and are fairly typical of nominally 99.9999% gold wire. It should be noted that, even without the oxygen and carbon, the measured impurity content of these wires was nearly two orders of magnitude larger than specified by the manufacturer.

The samples were heated in a $3\frac{1}{2}$-in. furnace to avoid "hot spots" which are frequently found with direct-resistance heating. The sample temperatures in the furnace were uniform to ± 3 °C over the 1-in. central sections of the sample on which measurements were made. The furnace has a slit on one side and was suspended about $\frac{1}{2}$ in. above a water bath at 20 °C. The samples were heated at 1050 °C in air for approximately 1 h and then quenched by dropping them from the furnace into the water bath. Temperatures were determined from the resistance of the wires.[21] Initially, the sample temperatures dropped ~75 °C at ~5 $\times 10^2$ °C/sec; during this slow temperature drop, the samples were passing through the insulation jacket of the furnace. When the samples reached the water bath, the temperature dropped to ambience at a rate of about 3×10^4 °C/sec.

Bass[22] has found that 16-mil gold samples, slow quenched in air 700–1000 °C, show quenched-in resistances which are essentially independent of the quenching temperature. The quenched-in re-

TABLE I. Mass spectrographic impurity analysis of gold samples used; all numbers in ppm by number of atoms.

Cu	Fe	Cr	Ti	Ca	K	Si	Al	Mg	Na	O	C
1.1	3.6	1.4	1.6	0.7	3.0	2.5	2.1	1.1	2.0	47	20

sistance of samples slow quenched from 1000 °C is much below that of samples fast quenched from the same temperature. During the initial stages of a slow quench, the vacancies are, evidently, sufficiently mobile that most of the excess anneals out. In our case, where the sample cooled relatively slowly to 975 °C, the vacancy concentration at the beginning of the fast water quench was probably close to the equilibrium concentration for samples at 975 °C, rather than to that at the furnace temperature. The quenched-in resistances of our samples were close to those obtained by Bass for quenches from 975 °C. However, we measured the resistance at room temperature whereas Bass made his measurements at 4 °K, so a direct comparison is difficult. The resistance of a vacancy may depend on temperature.[23,24] Therefore, the vacancy concentration in our samples may differ from Bass's.[22] This possible difference does not influence our results which do not depend for their interpretation on the actual defect concentrations.

After quenching, the samples were annealed in a large well-mixed bath of Eloxol No. 13 spark-cutter oil. The bath temperature was held constant to ±0.01 °C by means of a Fisher thermoregulator. Fluctuations in the bath temperature were measured with a Beckman differential thermometer, and the absolute bath temperature was measured with an N. B. S.-calibrated mercury thermometer.

The defect resistance of the sample was measured in the annealing bath using a simple differential technique originally developed by Bourassa *et al.*[14,15] In this method the sample to be quenched and a dummy of the same material are initially placed in the temperature-stabilized annealing bath. The sample and dummy are on the two sides of a differential circuit. The relative current in the two branches of the circuit is adjusted until the differential voltage drop is zero. The sample is then heated, quenched, and returned to the annealing bath. The differential voltage measured is then the voltage drop across the sample due to the resistivity and dimensional changes resulting solely from quenched-in defects. This circuit is usable only because the sample and dummy are maintained in the same annealing bath. Hence, the very small temperature fluctuations of the bath do not greatly affect the differential voltage drop. In practice, the noise in the differential voltage is about $\pm 2\times10^{-6}$ V, where V is the voltage drop across the sample. The differential voltage drifts at less than 1×10^{-6} V/h. The principal source of the noise in the differential voltage is the temperature fluctuations of the annealing bath. The differential voltage is partially offset with a μV potentiometer, and the deviation from the potentiometer null is followed on a photoelectric amplifier and chart recorder. This system makes it possible to measure the defect resistance to about $\pm 2\times10^{-6}R_0$, where R_0 is the sample resistance. Simultaneously, the defect resistance is plotted continuously as a function of time on a chart. The continuous plot of defect resistance on the chart paper is later digitalized for computer analysis of the data.

Activation energies were determined by the slope-change method using the continuous values derived for the time derivatives. To effect the small temperature step for this method, the sample was carefully removed from the annealing bath to avoid deformation and rapidly cooled to − 50 °C by suspending it over liquid nitrogen. The bath temperature was then changed to a new value and the sample was restored to the bath. This process required 10–15 min. When the cold sample was placed in the oil bath, the bath temperature was disturbed by about 0.1 °C. This temporary instability in the bath introduced considerable noise into the measured differential voltage. Therefore, data were not taken in the initial $1\frac{1}{2}$–2 min at the new temperature while the bath was recovering. It is clear that in future experiments it will be desirable to use two annealing baths to obviate such problems.

V. EXPERIMENTAL RESULTS

A. Annealing Kinetics

Quenched-in defects cause an increase in the resistance of the sample. This defect resistance then decays as the defects anneal out. In studying the annealing kinetics, it can be useful to neglect the permanent defects which do not anneal out under the experimental conditions. In this case, one

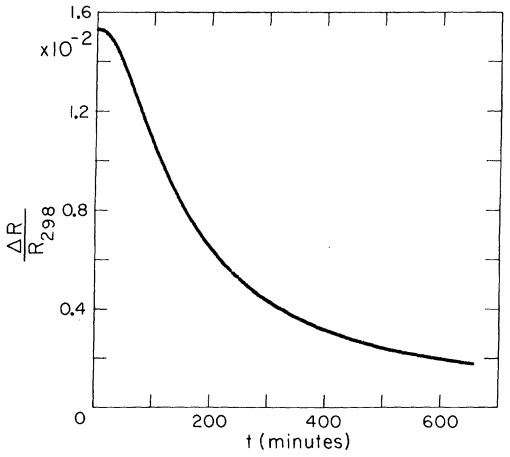

FIG. 5. Defect resistance ΔR divided by the sample resistance R_{298} versus time for a sample quenched from 975 °C and annealed at 30 °C.

examines not the defect resistance $\Delta\rho(t)$, but rather

$$\Delta R(t) = \Delta\rho(t) - \Delta\rho(\infty). \tag{12}$$

We shall, henceforth, call $\Delta R(t)$ the defect resistance and neglect those defects, such as tetrahedral stacking faults,[25,26] which do not anneal out at low temperatures.

Values for $\Delta R(t)$ are shown in Fig. 5 for a gold wire quenched from 975 °C and annealed at 30 °C. Figure 5 and others in this paper are actual plots of data points and not smooth curves drawn through the data points. The curve in Fig. 5 shows a typical S shape characteristic of the annealing of quenched gold.[9,27] Initially the annealing is slow, then speeds up, and then slows down again. This tendency is more evident in Fig. 6 where the time derivative $d\Delta R/dt$ is shown. Figure 6 was obtained by smoothing and differentiating the data shown in Fig. 5. Figure 7 shows $d^2\Delta R/dt^2$, the second derivative of the data shown in Fig. 5. For small times, the rate of increase of the annealing rate is found to be actually increasing.

The defect resistance $\Delta R(t)$ is plotted in Fig. 8 for another sample quenched from 975 °C and annealed at 70 °C. In this case, data were taken out to $40\tau_{1/2}$, where $\tau_{1/2}$ is the time for half the excess resistance to anneal out. Here the data show the hyperbolic shape characteristic of a second-order annealing process. For a second-order annealing process

$$\frac{d\Delta R}{dt} = -a(\Delta R)^2, \tag{13}$$

and hence,

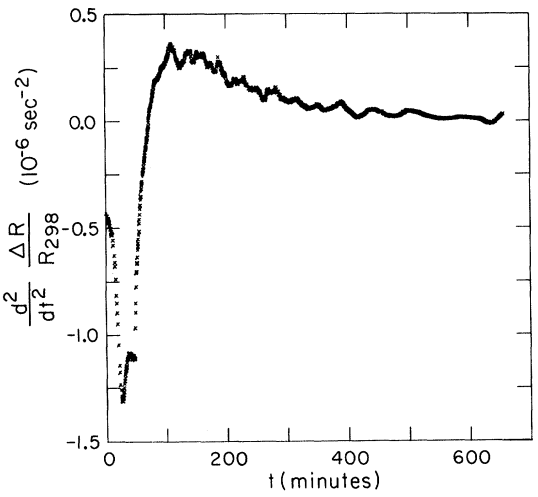

FIG. 7. $(d^2/dt^2)(\Delta R/R_{298})$ versus time obtained from the data in Fig. 6 by smoothing and differentiating.

$$\frac{1}{\Delta R}\frac{d\Delta R}{dt} = -a\Delta R, \tag{14}$$

where a is the second-order rate constant. For a pure second-order annealing process, a plot of $(1/\Delta R)(d\Delta R/dt)$ against ΔR should yield a straight line of slope $-a$. The function $(1/\Delta R)(d\Delta R/dt)$ is plotted against ΔR in Fig. 9; the original data are those shown in Fig. 8. For small times, the annealing is clearly not second order. This is also readily seen in the S-shaped curve of Fig. 5. For sufficiently long times, when most of the resistance is already annealed out, $(1/\Delta R)(d\Delta R/dt)$ as a function of ΔR is almost a straight line. However, there are small deviations. This is seen from the

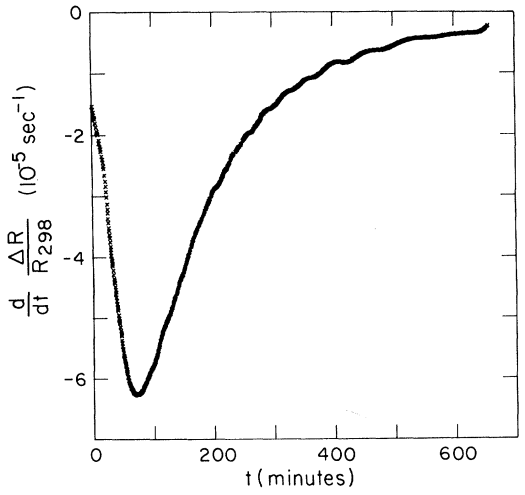

FIG. 6. $(d/dt)(\Delta R/R_{298})$ versus time obtained from the data in Fig. 5 by smoothing and differentiating.

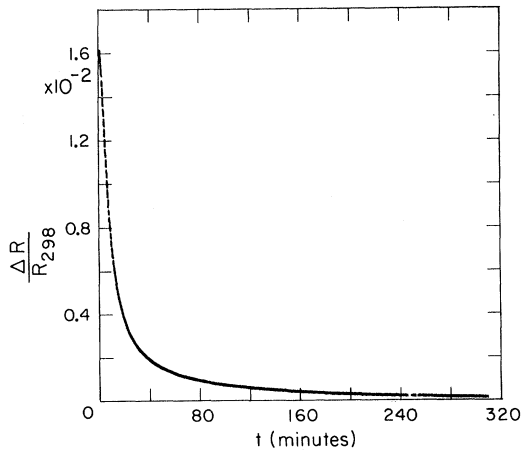

FIG. 8. Defect resistance ΔR divided by the sample resistance R_{298} versus time for a sample quenched from 975 °C and annealed at 70 °C.

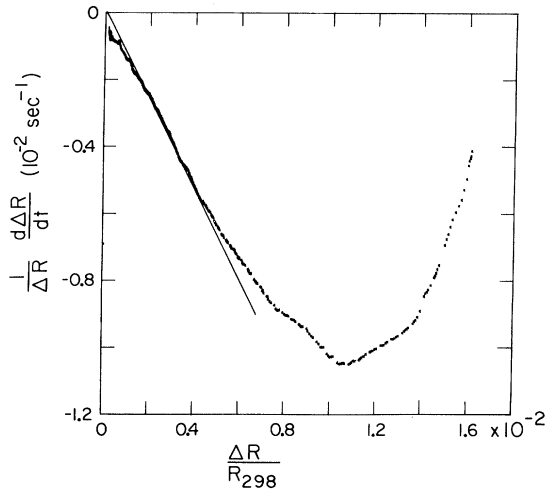

FIG. 9. $(d\Delta R/dt)/\Delta R/R_{298}$ for the data in Fig. 8. A straight line is drawn through the origin for comparison purposes.

straight reference line in the figure. Computer fitting of the data indicates that the deviations from a straight line are systematic. For this, and several other annealing curves carried almost to completion, the annealing was never found to be truly second order.

B. Activation Energies

Activation energies were obtained with Eq. (3) from the slope-change data. Data for one slope-change run are shown in Fig. 10. This sample was quenched from 975 °C and annealed at 37 °C until only 15% of the quenched-in defect resistance remained. At that time, the annealing temperature was changed from $T_1 = 37$ °C to $T_2 = 49$ °C. The annealing curve $\Delta R(t)$ at T_2 is plotted in Fig. 10(a). This curve was smoothed and differentiated to obtain $d\Delta R/dt$ plotted in Fig. 10(b). The time derivative is quite well determined. It is possible to obtain a value of $d\Delta R/dt(T_2, t_0)$ at the time of the temperature change by extrapolating $d\Delta R/dt$ backwards from large times. Two possible extrapolations are shown in Fig. 10(b). Clearly, the extrapolation is not well determined by these data. The value of $d\Delta R/dt(T_2, t_0)$ extrapolated from large times and used to derive E_{app} is quite different from the actual measured value near t_0 used to derive E_{inst}.

Using the actual values of $d\Delta R/dt$ near the time t_0 of the temperature change, we obtain values for E_{inst}. Figure 11 shows values computed for E_{inst} for one sample as a function of the fraction of the quenched-in resistance not yet annealed out. Detailed information about this run is in Table II.

The values of $d\Delta R/dt$ were corrected for a small apparent temperature dependence of the vacancy resistance. This correction was − 0.01 eV, which was smaller than the random errors. Random errors were estimated from the scatter of the derivative curves. The data in Fig. 11 are for one sample; other samples gave similar results. Qualitatively, E_{inst} is large initially and falls rapidly to a constant value of 0.52 ± 0.03 eV. Neglecting the initial annealing of the quenched-in defects, E_{inst} does not show any systematic dependence on either T_1 or T_2 or on whether T_1 is less than or greater than T_2. Activation energies close to this value have been observed previously by Koehler and co-workers.[3,9]

The extrapolations shown in Fig. 10 give a value of E_{app} between 0.70 and 0.95 eV. The apparent activation energy, characteristic of the rate-controlling annealing step, was even less well de-

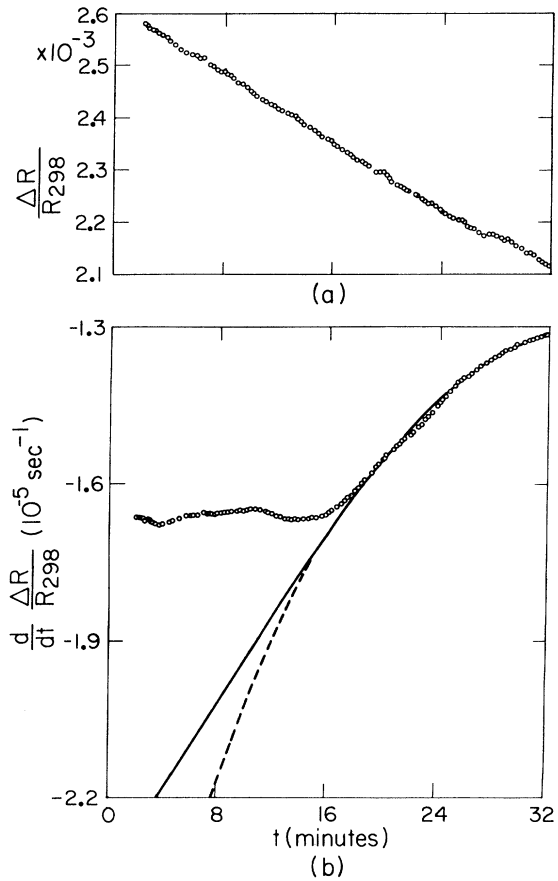

FIG. 10. Annealing curve after changing the sample temperature from 37 to 40 °C. (a) $\Delta R/R_{298}$ versus time; (b) $(d/dt)(\Delta R/R_{298})$ versus time obtained from (a) by smoothing and differentiating. Two possible extrapolations of $(d/dt)(\Delta R/R_{298})$ from long times to zero are indicated.

TABLE II. Details of the slope-change run for which activation energies are shown in Fig. 11. T is the temperature of the anneal and t is the time at temperature T. E_{inst} is the instantaneous activation energy obtained by slope change.

T (°C)	t (min)	E_{inst}(eV)
27.71	15	
		0.86 ± 0.04
37.48	15	
		0.56 ± 0.03
27.91	14	
		0.53 ± 0.02
37.98	15	
		0.48 ± 0.03
28.44	15	
		a
38.37	16	
		0.54 ± 0.02
28.21	20	
		0.53 ± 0.02
38.16	20	
		0.54 ± 0.02
28.53	30	
		0.55 ± 0.02
38.27	30	
		a
48.77	30	
		0.52 ± 0.02
37.15	40	
		0.47 ± 0.03
48.91	32	

[a]Energy not determined because of experimental difficulties.

termined for other annealing runs. Most of the runs were short and at low temperatures in order to obtain good values of the instantaneous activation energy. E_{app} could be obtained more precisely with long runs at higher temperatures.

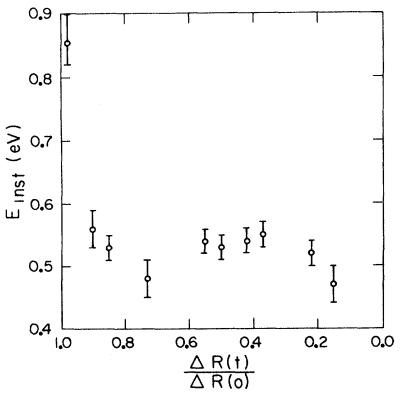

FIG. 11. Instantaneous activation energy E_{inst} versus fraction of quenched-in resistance remaining for a sample quenched from 975 °C. Detailed information about the run is in Table II.

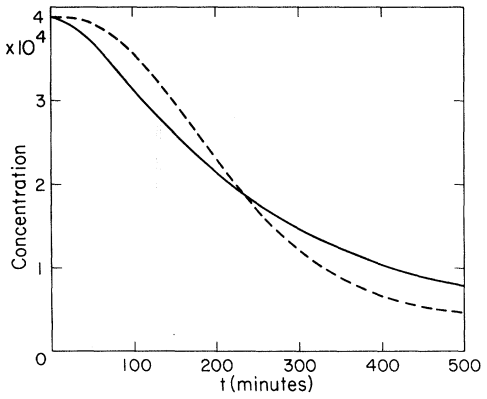

FIG. 12. R versus time for a model assuming fixed sinks (solid line) and a model assuming growing sinks (dashed line).

VI. DISCUSSION

In Sec. V we have found two new fundamental results for the annealing of gold quenched from high temperatures. We have the continuous first and second derivatives of the annealing curves and accurate values of the instantaneous activation energy. In the remainder of this paper, we shall examine a simple model which is consistent with the observed annealing curves and their derivatives. We shall also examine the instantaneous activation energy and ascertain its physical significance.

A. Annealing Kinetics

The standard reactions for the annealing of quenched gold were given in Eq. (4). These involve motion of single vacancies and divacancies to sinks and neglect higher-order defects and impurities. This model is not sufficient to explain tetrahedral-stacking fault formation,[25,26,28,29] but is qualitatively correct. This model is justified by the observation of approximately second-order kinetics for long times (Fig. 9) and the finding of annealing activation energies which clearly cannot correspond to single-vacancy motion.[12]

We have integrated the coupled differential equations [Eqs. (5)] arising from the reactions for $T = 30$ °C and an initial condition corresponding roughly to gold quenched from 975 °C.[20] Here, we assume

$$V_1(0) = 4 \times 10^{-4}, \quad V_2(0) = 0,$$

and use Eqs. (6) for k_1, k_2, k_{12}, and k_{21}. We have examined two models. Model 1 assumed a constant sink concentration, $S = 10^{-6}$ and $\nu = 4 \times 10^{14}$ min^{-1}. Model 2 assumed that the sink concentration increased proportionately to time, $S = 5 \times 10^{-9} t$ (in min) and $\nu = 5 \times 10^{14}$ min^{-1}. The value of ν was

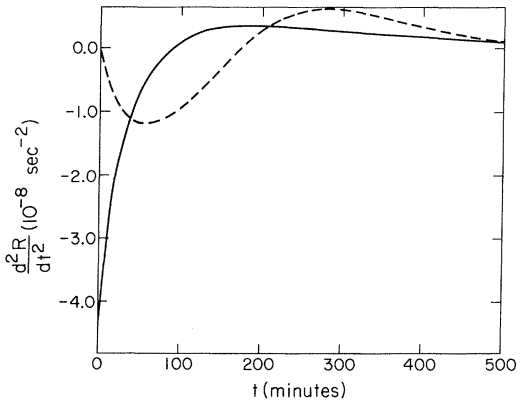

FIG. 13. d^2R/dt^2 versus time based on Fig. 8.

chosen to give computer-generated R-versus-t data similar to the experimental data. R is plotted versus t for both models in Fig. 12. Both plots are quite similar to the experimental data of Fig. 5. For both models, dR/dt is qualitatively similar to the experimental results. However, the second derivatives d^2R/dt^2, shown in Fig. 13, are qualitatively similar to the experimental results, Fig. 7, assuming sinks which grow during the anneals (dashed curve) but are dissimilar assuming constant sinks (solid curve). This agreement, assuming growing sinks, is physically reasonable. There is considerable experimental evidence that tetrahedral-stacking faults nucleate during the initial stages of annealing and grow subsequently.[25,26]

The behavior of d^2R/dt^2 for both models is similar to the experimental result for large times. Hence, it is important to determine whether the number of sinks continues to increase at large times or only increases for a short initial time period. However, the qualitative agreement between experimental results and model is encouraging.

In Fig. 9, we showed that dR/dt is not experimentally exactly second order in R. Neither of our models gives strictly second-order annealing kinetics. The value of $(1/R^2)(dR/dt)$ is plotted as a function of time in Fig. 14 for the fixed-sink model and becomes approximately constant only for annealing times greater than roughly $30\tau_{1/2}$.

B. Activation Energy

In Sec. VI A, we have found that the usual model of the annealing of quenched gold which involves single vacancies, divacancies, and sinks,[17,18] can satisfactorily account for the observed annealing curves, provided the sink concentration is increasing at small times. We now wish to use this single-divacancy model to understand the observed activation energies.

The experimental instantaneous activation energies E_{inst} are plotted in Fig. 11. After a brief initialization period, E_{inst} becomes constant at 0.52 ± 0.03 eV. This energy clearly cannot be a single-vacancy-motion energy: When this value is added to the (approximate single-vacancy-formation energy of 0.95 eV,[20,30] the sum 1.47 eV is far smaller than the experimentally determined activation energy for gold self-diffusion 1.83 eV.[31] The instantaneous activation energy must be characteristic of some basic defect motion, since it is determined by the defect-annihilating step in the recovery process. The obvious choice is the divacancy. In the models which give qualitative agreement with experiment, both single vacancies and divacancies annihilate. If divacancies are much more mobile than single vacancies, E_{inst} should be essentially equal to E_2^m the divacancy-motion energy.

Activation energies near 0.52 eV have been observed previously but have not been interpreted as the divacancy-motion energy. Koehler and coworkers[3,9] observed activation energies only slightly larger than 0.52 eV for gold samples fast quenched from high temperatures. These activation energies were determined by conventional slope-change methods and did not distinguish between the instantaneous and apparent activation energies. Bauerle and Koehler[9] annealed approximately 6 min at temperatures of 30 and 40 °C and obtained activation energies between 0.53 and 0.69 eV. de Jong and Koehler[3] also annealed at 30 and 40 °C and found a time dependence of the activation energy. They found energies which increased from 0.55 to 0.69 eV, while the time at the annealing temperature was increased from less than 30 min to 10 h. In short anneals, conventional slope change can give activation energies comparable to E_{inst}. However, with long anneals conventional slope-change methods could give a higher value of

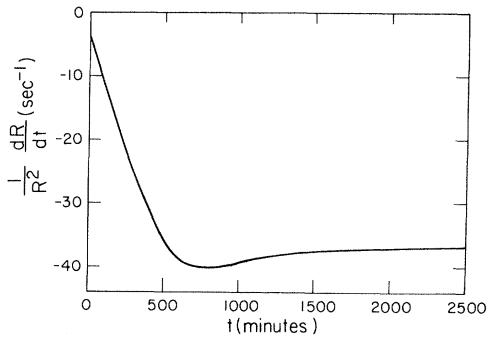

FIG. 14. $(1/R^2)(dR/dt)$ versus time for a model assuming fixed sinks.

the activation energy, since the single vacancies and divacancies can approach a steady state.

The low activation energy was interpreted by de Jong and Koehler as being $E_2^m - B_2$, when B_2 is the divacancy-binding energy. They arrived at this conclusion by assuming that single vacancies and divacancies are always in equilibrium. This assumption is not in agreement with either our observed difference between E_{inst} and E_{app} or with their own changing value of the activation energy. Our computer simulations of the slope-change process clearly show the effects of reequilibration of single vacancies and divacancies (Fig. 4). The new value of the divacancy-motion energy of 0.52 eV is significantly smaller than the previously accepted value of 0.70 eV.[12]

From our results, the instantaneous activation energy is found initially to be considerably larger than 0.52 eV. During this initialization period, sinks are growing and the divacancy concentration is increasing rapidly. The interpretation of E_{inst} during this complicated initialization period is uncertain.

We have made one evaluation of the apparent activation energy, which is determined by the rate-controlling annealing step. From extrapolation for long times after t_0, E_{app} is found to be between 0.70 and 0.95 eV. This is the range of activation energies found by most other experimenters using more conventional techniques.[12,17,18] Further experiments to determine E_{app} much more accurately may give more insight into the microscopic atomic processes in annealing of quenched gold. The absence at this time of additional data using the new measuring technique makes it unfruitful to speculate on the interpretation of other activation energies obtained in earlier experiments.

VII. CONCLUSIONS

In this paper, we have shown that conventional slope-change activation energy measurements do not necessarily yield physically significant results in quenching experiments because of transient effects. There actually exist two activation energies: the instantaneous energy characteristic of the defect-annihilation step and the apparent activation energy characteristic of the rate-controlling step. Measurement of these two activation energies requires continuous time derivatives of the defect concentrations.

We have examined the resistivity annealing of high-purity gold quenched from 975 °C. We have used a new technique which gives the defect resistance continuously and which allows us to obtain first- and second-time derivatives of the resistance.

We have examined the second-time derivative of the resistance-annealing curves and have shown that it is compatible with a model involving single vacancies, divacancies, and a concentration of sinks which increases with time, at least for small times. The data are not consistent with a fixed-sink concentration.

We have shown that the instantaneous activation energy is 0.52 ± 0.03 eV and that this value is most probably indentifiable with the divacancy-motion energy.

ACKNOWLEDGMENTS

The authors are grateful to Dr. R. K. Sharma and Professor J. S. Koehler for communication of their results prior to publication, and for several illuminating discussions of the annealing kinetics.

---

†Research supported in part by the U.S. Atomic Energy Commission under Contract No. AT(11-1)-1198.

*Present address: Henry Krumb School of Mines, Columbia University, New York, N.Y. 10027.

[1]J. S. Koehler, F. Seitz, and J. E. Bauerle, Phys. Rev. 107, 1499 (1957).

[2]J. S. Koehler, M. de Jong, and F. Seitz, J. Phys. Soc. Japan, Suppl. 18, 1 (1963).

[3]M. de Jong and J. S. Koehler, Phys. Rev. 129, 40 (1963).

[4]M. Doyama, Phys. Rev. 148, 681 (1966); R. K. Sharma and J. S. Koehler, Phys. Rev. (to be published).

[5]R. A. Johnson, Phys. Rev. 174, 691 (1968).

[6]A. C. Damask and G. J. Dienes, *Point Defects in Metals* (Gordon and Breach, New York, 1963), p. 145.

[7]R. W. Balluffi and R. W. Siegel, in *Lattice Defects in Quenched Metals*, edited by R. M. J. Cotterill, M. Doyama, J. J. Jackson, and M. Meshii (Academic, New York, 1965), p. 693.

[8]M. Doyama, in Ref. 7, p. 167.

[9]J. E. Bauerle and J. S. Koehler, Phys. Rev. 107, 1493 (1957).

[10]J. W. Kauffman and J. S. Koehler, Phys. Rev. 88, 149 (1952).

[11]A number of papers on this topic and extensive references may be found in Ref. 7.

[12]C. G. Wang, D. N. Seidman, and R. W. Balluffi, Phys. Rev. 169, 553 (1968).

[13]A. Seeger and H. Mehrer, Phys. Status Solidi 29, 231 (1968).

[14]R. R. Bourassa, Ph.D. thesis, University of Illinois, 1967 (unpublished).

[15]R. R. Bourassa, D. Lazarus, and D. A. Blackburn, Phys. Rev. 165, 853 (1968).

[16]J. J. Burton and D. Lazarus, Appl. Phys. Letters 16, 131 (1970).
[17]J. W. Kauffman and M. Meshii, in Ref. 7, p. 77 ff.
[18]T. Kino and J. S. Koehler, Phys. Rev. 162, 632 (1967).
[19]ν is not well known and appears in these equations only as a multiplicative constant which determines the time scale.
[20]R. O. Simmons and R. W. Balluffi, Phys. Rev. 125, 862 (1962).
[21]C. J. Meechan and R. R. Eggleston, Acta Met. 2, 680 (1954).
[22]J. Bass, Phys. Rev. 137, A765 (1965).
[23]R. R. Conte and J. Dural, Phys. Letters 27A, 368 1968).
[24]J. S. Zetts, R. P. Gripshover, and J. Bass, Phys. Letters 29A, 255 (1969).
[25]J. Silcox and P. B. Hirsch, Phil. Mag. 4, 72 (1959).
[26]K. P. Chik, Phys. Status Solidi 10, 659 (1965).
[27]R. W. Siegel, Phil. Mag. 13, 337 (1966).
[28]M. de Jong and J. S. Koehler, Phys. Rev. 129, 49 (1963).
[29]K. P. Chik, Phys. Status Solidi 10, 675 (1965).
[30]W. DeSorbo, Phys. Rev. 117, 444 (1960).
[31]H. M. Gilder and D. Lazarus, J. Phys. Chem. Solids 26, 208 (1965).

PHYSICAL REVIEW B VOLUME 2, NUMBER 4 15 AUGUST 1970

Plasma Effects on Transition Radiation from Metal Foils*

T. K. Bolland†
Department of Physics, Lehigh University, Bethlehem, Pennsylvania 18015
(Received 18 June 1969)

The transition radiation emitted from a thin metal foil bombarded by electrons is calculated, taking into account the excitation of plasma waves in the foil. The correction the plasma waves introduce varies greatly in different cases and can be of the order of 10% or greater at the frequency at which the radiation has its peak intensity.

I. INTRODUCTION

Transition radiation is the radiation emitted due to the passage of a charged particle through an inhomogeneous medium, for example, as in crossing the boundary between two media of different dielectric constants. This radiation, first discussed by Frank and Ginzburg[1] in 1945, has been the subject of increasing interest in recent years.

The transition radiation is a consequence of the boundary conditions appropriate to the given situation. To calculate the transition radiation, one applies these conditions to the fields at the boundary crossed by the particle, while the media on either side of the boundary are described in some suitable way.

Problems in electromagnetic theory involving boundaries, such as transition radiation or the derivation of Fresnel's formulas, are usually worked under the assumption that the media in question are described by their dielectric constants, permeabilities, or refractive indices. Recently, Sauter[2] pointed out that this approach failed to take into account the possibility of excitation of plasma waves in the case of metals, so that, for instance, there should be corrections to Fresnel's formula for the reflection coefficient of a metal surface in certain circumstances.

It is of interest to consider what effect these plasma waves would have on transition radiation, since the targets usually used for experimental investigations are thin foils of aluminum, silver, or similar metals. Forstmann[3] has done such a calculation for electrons incident (obliquely) from vacuum on a semi-infinite metal. This paper reports the calculations for a thin metallic film.

II. FUNDAMENTAL EQUATIONS

The equation of motion of a degenerate electron gas in the metal is given by

$$\dot{\vec{v}}(\vec{r},t)+f\vec{v}(\vec{r},t)=-\frac{e}{m}\vec{E}(\vec{r},t)-\frac{W^2}{n_0}\nabla n(\vec{r},t)\ , \quad (1)$$

where the constant $W^2=\frac{3}{5}v_F^2$ for a completely degenerate electron gas with a Fermi velocity v_F. Further, $\vec{v}$ is the velocity of an element of the electron gas, n_0 is the equilibrium number density of the electrons (and constant density of the positive ions), n is the deviation of the electron number density from n_0, $-e/m$ is the charge to mass ratio of an electron, f is the inverse of the relaxation time of the electrons, and $\vec{E}$ is the total electric field inside the metal. Assume that $n \ll n_0$.